0013-7227/05/$15.00/0
Printed in U.S.A.

Endocrinology 146(4):1893–1908

doi: 10.1210/en.2004-1464

Blood-Testis Barrier Dynamics Are Regulated by α_2-Macroglobulin via the c-Jun N-Terminal Protein Kinase Pathway

Ching-hang Wong, Dolores D. Mruk, Michelle K. Y. Siu, and C. Yan Cheng

Population Council, New York, New York 10021

The blood-testis barrier (BTB), in contrast to the blood-brain and blood-retina barriers, is composed of coexisting tight junctions, gap junctions, and basal ectoplasmic specializations, a testis-specific type of adherens junction. Recent studies showed that BTB restructuring that facilitates germ cell migration during spermatogenesis involves proteolysis, an event that is usually restricted to the cell-matrix interface in other epithelia. For instance, a surge in α_2-macroglobulin (α_2-MG), a protease inhibitor produced by Sertoli cells, was detected at the Sertoli-Sertoli and Sertoli-germ cell interface in the epithelium during cadmium chloride-induced BTB disruption in adult rats. It is thus proposed that the increase in α_2-MG is crucial for protecting the epithelium from unwanted proteolysis as well as regulating the availability of cytokines that affect junction turnover. Although both tight junction and adherens junction dynamics at the BTB are regulated via the p38 MAPK signaling pathway, the mechanism(s) that regulates α_2-MG is entirely unknown. In this study, we have shown that by administering dimethylaminopurine, a c-Jun N-terminal protein kinase (JNK) inhibitor, to the testis, JNK activity was blocked specifically and α_2-MG production was inhibited, worsening the cadmium chloride-induced damage to the epithelium. Studies coupled with inhibitors, immunoblottings, and immunofluorescent and electron microscopy have unequivocally demonstrated that the JNK signaling pathway is a putative regulatory pathway for α_2-MG production in the testis. This finding illustrates for the first time that a cell-matrix restructuring event occurs in normal cell physiology at the cell-cell interface in the testis, highlighting the significance of α_2-MG in the regulation of BTB function. (*Endocrinology* 146: 1893–1908, 2005)

PROTEOLYSIS IS AN important event in tissue remodeling and cell migration (for reviews, see Refs. 1 and 2), but it usually is restricted to cell-matrix interface under normal physiological conditions. In pathophysiological responses, such as inflammation when neutrophils transmigrate across the vascular endothelial tight junction (TJ) barrier, proteolysis can be detected at cell-cell contact sites (3). Interestingly, recent studies implicated the involvement of proteolysis at the cell-cell interface in the seminiferous epithelium during spermatogenesis (4–7, for reviews, see Refs. 8–10). However, how they participate in junction restructuring and how their activities are regulated during spermatogenesis are still not fully understood.

α_2-Macroglobulin (α_2-MG), a 720-kDa glycoprotein consisting of four identical 180-kDa subunits, is among one of the earliest protease inhibitors discovered in the testis (for a review, see Ref. 8). In the systemic circulation, α_2-MG is an acute-phase protein produced by hepatocytes, inhibiting all classes of proteases via an entrapment mechanism (for a review, see Ref. 11). It binds to TGFβ (12) and other growth factors and hormones with high affinity (for reviews, see Refs. 13 and 14). In the seminiferous epithelium behind the blood-testis barrier (BTB), α_2-MG, but not germ cells, is a secretory product of Sertoli cells (15). It was localized to Sertoli cell cytoplasm and around the heads of elongating and elongate spermatids in the rat testis possibly at the site of apical ectoplasmic specialization (ES), suggestive of its significance in germ cell movement and spermiation (7). It was postulated that α_2-MG might limit unwanted proteolysis as a result of extensive tissue remodeling in the seminiferous epithelium pertinent to spermatogenesis (7). Indeed, recent *in vitro* studies demonstrated that this protease inhibitor, working in concert with other proteases, facilitates the attachment of germ cell onto the Sertoli cell epithelium (4, 10), illustrating its role in adherens junction (AJ) assembly.

The involvement of α_2-MG in junction restructuring, particularly at the BTB *in vivo*, was unequivocally demonstrated in a recent study using cadmium chloride ($CdCl_2$)-induced BTB damage as a model to study junction dynamics (6). For instance, a primary disruption of Sertoli cell TJs at the BTB induced by $CdCl_2$ administration (3 mg/kg body weight, ip) could lead to a secondary damage of both basal and apical ES in the seminiferous epithelium. This in turn led to germ cell loss from the epithelium. Interestingly, α_2-MG in the seminiferous epithelium was induced significantly and was localized to the BTB site (*i.e.* Sertoli-Sertoli TJ and basal ES) as well as the heads of detaching spermatids at the apical ES

First Published Online December 23, 2004

Abbreviations: AJ, Adherens junction; BTB, blood-testis barrier; $CdCl_2$, cadmium chloride; DMAP, 6-dimethylaminopurine; DMSO, dimethylsulfoxide; er, ectoplasmic reticulum; ES, ectoplasmic specialization; FITC, fluorescein isothiocyanate; i.t., intratesticularly; JNK, c-Jun N-terminal protein kinase; α_2-MG, α_2-macroglobulin; MEK, MAPK/ERK kinase; MMP, matrix metalloprotease; p-ERK, phospho-ERK; SB202190, 4-(4-fluorophenyl)-2-(4-hydroxyphenyl)-5-(4-pyridyl)1H-imidazole; SDS, sodium dodecyl sulfate; ST, seminiferous tubule; T, total acrylamide concentration (g/100 ml) = acrylamide + bisacrylamide; TJ, tight junction; U0126, 1,4-diamino-2,3-dicyano-1,4-bis(2-aminophenylthio)butadiene; ZO-1, zonula occludens-1.

***Endocrinology* is published monthly by The Endocrine Society (http://www.endo-society.org), the foremost professional society serving the endocrine community.**

site (6). These findings strengthen the notion that α_2-MG protects the seminiferous epithelium from excessive damage pertinent to junction restructuring during spermatogenesis. However, whereas the protein levels of occludin, zonula occludens-1 (ZO-1), cadherins, and nectins in the seminiferous epithelium were shown to be regulated by TGFβ3 via the p38 MAPK pathway during $CdCl_2$-induced BTB disruption (6, 16), α_2-MG was not regulated via this pathway.

We have now identified the signaling pathway that regulates α_2-MG homeostasis in the testis. We have also determined whether a blockade of α_2-MG production in the seminiferous epithelium by using specific inhibitors can worsen the $CdCl_2$-induced damage in the epithelium. It is apparent that the opening and closing of the BTB is regulated by two independent but possibly interrelated signaling pathways, namely the p38 MAPK and the c-Jun N-terminal protein kinase (JNK) pathways, which regulate the homeostasis of junction-associated proteins and proteases, and protease inhibitors, respectively.

Materials and Methods

Animals

Male Sprague Dawley rats (outbred) were purchased from Charles River Laboratories (Kingston, NY). All animals were kept at the Rockefeller University Laboratory Animal Research Center (New York, NY). The use of animals reported in this paper was approved by The Rockefeller University Animal Care and Use Committee (protocol no. 97113, 00111, and 03017).

Reagents

Apigenin (4′,5,7-trihydroxyflavone), DMAP (6-dimethylaminopurine) and SB202190 [4-(4-fluorophenyl)-2-(4-hydroxyphenyl)-5-(4-pyridyl)1H-imidazole] were purchased from Calbiochem (La Jolla, CA). U0126 [1,4-diamino-2,3-dicyano-1,4-bis(2-aminophenylthio)butadiene] was from Cell Signaling Technology (Beverly, MA). A polyclonal antibody against α_2-MG purified from Sertoli cell-enriched culture medium was prepared in a rabbit and characterized earlier from this laboratory (15). Goat antiactin (catalog no. sc-1616, lot E0503) and rabbit anti-β-catenin (catalog no. sc-7199, lot D171) were purchased from Santa Cruz Biotechnology (Santa Cruz, CA). Mouse anti-Cdc42 (catalog no. 610842, lot 5) and anti-E-cadherin antibodies (catalog no. 610181, lot 9) were obtained from BD Transduction Laboratories (San Diego, CA). Rabbit anti-JNK (catalog no. 9252, lot 4), anti-phospho-p38 MAPK (catalog no. 9211, lot 3), anti-phospho-ERK (p-ERK) (catalog no. 9101, lot 15), anti-c-Jun (catalog no. 9126, lot 9), and mouse anti-phospho-JNK antibodies (catalog no. 9255, lot 10) were purchased from Cell Signaling Technology. Rabbit antioccludin (catalog no. 71-1500, lot 11067632), anti-ZO-1 (catalog no. 61-7300, lot 30175033), anti-β-catenin (for immunofluorescent staining, catalog no. 71-2700, lot 30477187), mouse anti-ZO-1 IgG-fluorescein isothiocyanate (FITC) (catalog no. 33-9100, lot 20269234), anti-*N*-cadherin (catalog no. 33-3900, lot 21073914), goat antirabbit IgG-Cy-3 and goat antimouse IgG-FITC were from Zymed Laboratories (San Francisco, CA). Horseradish peroxidase-conjugated secondary antibodies used in immunoblotting were obtained from Santa Cruz Biotechnology. The JNK/stress-activated protein kinase assay kit was purchased from Cell Signaling Technology. Histostain-SP kit for immunohistochemistry was from Zymed Laboratories.

Experimental design

The goal of this study was to define the role of proteolysis in BTB restructuring pertinent to spermatogenesis using α_2-MG as a marker protein and delineate the signaling pathway that regulated α_2-MG production in the seminiferous epithelium. We used an *in vivo* model of BTB restructuring in which the Sertoli cell TJ permeability barrier and the microvascular endothelial TJ barrier were compromised by cadmium toxicity in a time-dependent manner. The kinetics of their disruption were monitored by light and electron microscopy after treatment of adult rats with $CdCl_2$ at 3 mg/kg body weight, administered via ip injection, and rats were terminated at 1, 3, 5, 7, 12, 16, 20, 24, 48, and 96 h thereafter. It was noted that the Sertoli cell TJ barrier was the primary target of cadmium toxicity in the testis, and it was disrupted at least 10–14 h before any signs of microvascular TJ barrier damage was detected by electron microscopy. As such, many of the detected changes in target proteins pertinent to signal transduction in the testis are the results of BTB restructuring induced by $CdCl_2$ instead of secondary to anoxia because of the microvessel damage. Using this approach, the steady-state levels of MAPKs including their activated forms (*e.g.* phospho-JNK) and the upstream signal transducers (*e.g.* Cdc42) were quantified by immunoblottings. When the induction of a MAPK was detected, the authenticity of its activation was confirmed by a specific intrinsic kinase assay. This was followed by studies using inhibitors to demonstrate whether the presence of a specific inhibitor (*e.g.* DMAP that blocks JNK activity) could indeed block (or significantly reduce) the expression of a target protein (*e.g.* α_2-MG). Thereafter the inhibitor was used to examine whether it could worsen the cadmium-induced damage to the seminiferous epithelium in the testis, such as the integrity of the BTB and the Sertoli-germ cell AJs, using techniques of fluorescent microscopy and immunoblottings to yield semiquantitative data. The following sections are brief descriptions of different techniques used for experiments described in this report.

Disruption of BTB in vivo by $CdCl_2$

BTB damage in rat testes was induced by $CdCl_2$ as described (6, 17, 18). In brief, $CdCl_2$ was prepared in 0.1% solution (wt/vol, in MilliQ H_2O), and administered via ip to groups of rats with body weights ranging between 250 and 330 g (n = 3–5 rats per time point) at 3 mg/kg body weight. Rats were killed at specified time points after $CdCl_2$ treatment by CO_2 asphyxiation, and testes were immediately removed, frozen in liquid nitrogen, and store at −80 C until used.

Pretreatment of rats with MAPK inhibitors before $CdCl_2$ exposure

To assess the effects of MAPK inhibitors on $CdCl_2$-induced BTB damage, one of the testes from each rat (n = 3–4 rats) was injected intratesticularly (i.t.) with one of the following inhibitors before $CdCl_2$ treatment (3 mg/kg body weight, ip): apigenin, DMAP, SB202190, and U0126, as described (19–21). The other testis of the same rat served as a control, receiving vehicle alone (see Table 1). Preparations of inhibitors are summarized in Table 1. All inhibitors were first dissolved in either dimethylsulfoxide (DMSO) or sterile H_2O and then diluted to desired concentration in approximately 200 μl sterile saline (0.89% NaCl wt/vol in MilliQ water). An approximately 70-μl sample was administered per site using a 27-gauge needle to a total of three sites per testis. Thereafter animals received a single dose of $CdCl_2$ (3 mg/kg body weight) via ip to induce BTB damage to examine the effects of different inhibitors on changes in α_2-MG and other junction-associated proteins. Rats were

TABLE 1. Preparation of MAPK inhibitors for intratesticular administration to adult rats

Inhibitor	Concentration used	Solvent used	Corresponding vehicle control	Mode of action
Apigenin	1 μM (1.6 nmol)[a]	DMSO	0.2% DMSO in saline	An inhibitor of all MAPKs
DMAP	5 mM (8 μmol)	H_2O	Saline	A specific JNK inhibitor
SB202190	5 μM (8 nmol)	DMSO	1% DMSO in saline	A specific p38 MAPK inhibitor
U0126	100 μM (160 nmol)	DMSO	1% DMSO in saline	A specific MEK/ERK inhibitor

[a] This is the amount of inhibitor administered per testis via intratesticular injection using a 27-gauge needle in which the volume of each testis was estimated to be approximately 1.6 ml.

killed 16 h after $CdCl_2$ treatment unless specified otherwise, and testes were collected, frozen in liquid nitrogen, and stored at −80 C.

Immunoblotting

Immunoblot analyses were performed using testes lysates prepared in sodium dodecyl sulfate (SDS) lysis buffer [0.125 M Tris (pH 6.8) at 22 C containing 1% SDS (wt/vol), 2 mM EDTA, 2 mM *N*-ethylmaleimide, 2 mM phenylmethylsulfonyl fluoride, 1.6% 2-mercaptoethanol (vol/vol), 1 mM sodium orthovanadate, and 0.1 μM sodium okadate]. An equal amount of proteins from lysates (~100 μg) was resolved by SDS-PAGE under reducing conditions. Proteins were electroblotted onto nitrocellulose membranes and probed with one of the following primary antibodies at the denoted dilution: α_2-MG (1:750), Cdc42 (1:1000), JNK (1:1000), phospho-JNK (1:2000), actin (1:200), phospho-p38 MAPK (1:1000), p-ERK (1:1000), occludin (1:250), ZO-1 (1:250), N-cadherin (1:250), E-cadherin (1:2500), and β-catenin (1:200). The working dilution of primary antibodies was selected based on preliminary experiments. Different horseradish peroxidase-conjugated secondary antibodies (1:2000) were used based on the origins of primary antibodies. Target proteins on nitrocellulose membranes were visualized by enhanced chemiluminescence as described (6). Each immunoblotting experiment was repeated at least three times using different sets of samples to obtain data for statistical analysis.

JNK activity assay

The intrinsic JNK activity in testes during $CdCl_2$-induced BTB damage was quantified using a nonradioactive assay. In brief, lysates from testes after treatments were prepared using a lysis buffer [20 mM Tris (pH 7.5), at 22 C containing 150 mM NaCl, 1 mM EDTA, 1 mM EGTA, 1% Triton (vol/vol), 2.5 mM sodium pyrophosphate, 1 mM β-glycerolphosphate, 1 mM sodium orthovanadate, 1 μg/ml leupeptin, and 1 mM phenylmethylsulfonyl fluoride]. JNK in approximately 250 μg of proteins in each sample lysate was pulled down selectively by an N-terminal c-Jun (residues 1–89) fusion protein that were bound to glutathione-Sepharose beads at 4 C overnight with gentle agitation. All samples within an experimental group were processed and assayed in the same experimental session to eliminate interassay variations. Thereafter beads were washed twice with the lysis buffer and twice with a kinase buffer [5 mM Tris (pH 7.5), at 22 C containing 5 mM glycerolphosphate, 2 mM dithiothreitol, 0.1 mM sodium orthovanadate, and 10 mM $MgCl_2$]. Kinase reactions were then carried out at 30 C for 30 min in the presence of 100 μM cold ATP, during which c-Jun fusion proteins were phosphorylated by the activated JNK. c-Jun phosphorylations were subsequently detected by immunoblotting using a specific phospho-c-Jun (Ser-63) antibody. The same blot was stripped and reprobed with a c-Jun antibody to monitor equal loading of fusion proteins.

A morphological study to assess the effects of DMAP pretreatment on the kinetics of germ cell loss from the seminiferous epithelium and microvascular TJ barrier disruption induced by cadmium toxicity

To examine the effects of DMAP pretreatment that blocked the intrinsic JNK kinase activity on $CdCl_2$-induced damage on the morphology of rat testes, rats received DMAP via i.t. injection (see Table 1 for amount used) following by $CdCl_2$ (3 mg/kg body weight, ip) were terminated at specified time points: 0, 5, 10, 14, 16, and 20 h. Testes were removed and fixed in Bouin's fixative, embedded in paraffin, sectioned, and stained with hematoxylin and eosin. Cross-sections of testes were examined by a BX-40 microscope (Olympus Corp., Melville, NY). All images were acquired using an Olympus DP70 12.5MPa digital camera interfaced to an Vectra VL800 workstation (Hewlett Packard, Palo Alto, CA) via Firewire using the QCapture Suite software package (version 2.60, Quantitative Imaging Corp., Burnaby, British Columbia, Canada). To further compare the differences between normal rats and the treatment groups, the number of seminiferous tubules in the testis sections with abnormal germ cell distribution, which is classified by germ cells prematurely detached from the epithelium and found in the tubule lumen, and/or tubules with empty patches in the epithelium indicating losses of maturing germ cells, was tallied. It is noted that in normal testes, only fully mature spermatids (spermatozoa) were found in the lumen at late stage VIII of the epithelial cycle. The percentage of normal seminiferous tubules (STs) at each time point within a treatment group was calculated as follows:

$$\{[\mathrm{ST(total)} - \mathrm{ST(abnormal\ germ\ cell\ distribution)}]/\mathrm{ST(total)}\} \times 100\%$$

where ST(total) represents the total number of tubules tallied and ST(abnormal germ cell distribution) represents tubules with an abnormal germ cell distribution. In this experiment, we also estimated microvascular TJ barrier damage by observing tubules with erythrocytes in the interstitium, which was associated with disruptions of microvascular TJs. About 200 cross-sections of tubules per testis were scored and the mean ± SD was computed from three different rats at each time point in each treatment group.

Electron microscopy

Electron microscopy was performed as described (6). In brief, rats were treated with DMAP and/or $CdCl_2$ as described above. Rats without $CdCl_2$ treatment served as controls. Testes collected immediately after rats were killed by CO_2 asphyxiation were immersed in 2.5% glutaraldehyde/0.1 M sodium cacodylate (pH 7.4, 22 C) and incised to release the seminiferous tubules and blood capillaries. Tissues were fixed for 2–4 h at room temperature, to be followed by postfixation in 1% OsO_4 solution and stained in 1% uranyl acetate. Tissues were then dehydrated in ascending concentrations of ethanol, incubated in propylene oxide, and infiltrated with EMbed (Electron Microscopy Sciences, Fort Washington, PA). After overnight infiltration, EMbed was discarded and replaced with fresh solution, and the whole specimen was incubated in Embed at 60 C for 2 d. Ultrathin (~80 nm) sections were cut on a Reichert-Jung Ultracut E microtome (Bannockburn, IL) and poststained with uranyl acetate/lead. Sections were examined and photographed on a JEOL 100CXII electron microscope (Peabody, CA) at 80 kV.

Localization of α_2-MG in the rat testis by immunohistochemistry

Immunohistochemical localization of α_2-MG in the rat seminiferous epithelium after different treatments *vs.* normal rats was essentially performed as earlier described (6, 7). All cross-sections of testes within an experimental group were processed simultaneously in the same experimental session by placing five to six cross-section per slide to eliminate interexperimental differences during color development. Immunoreactive α_2-MG appeared as reddish brown precipitates. Controls included sections incubated with the following: 1) a preimmune serum instead of the primary α_2-MG antiserum, 2) PBS in substitution of the primary antibody, and 3) normal goat serum replacing the secondary antibody.

Immunofluorescent microscopy

Fluorescent microscopy was used to assess damages to TJs and basal ES at the BTB by colocalizations of occludin with ZO-1, and N-cadherin with β-catenin, using testes from normal rats and rats in different treatment groups. In brief, frozen sections of testes were fixed in Bouin's fixative, and nonspecific binding sites were blocked with 10% normal goat serum. In colocalization of occludin and ZO-1, sections were incubated with a rabbit antioccludin antibody (1:100) followed by a goat antirabbit IgG-Cy-3, and a mouse anti-ZO-1 IgG-FITC (1:100). For N-cadherin/β-catenin staining, sections were incubated with a mouse anti-N-cadherin (1:100) and a rabbit anti-β-catenin (1:100), which was followed by a goat antimouse IgG-FITC and a goat antirabbit IgG-Cy3. Sections were then washed, mounted in Vectashield Hardset with 4′,6′-diamino-2-phenylindole (DAPI) (Vector Laboratories, Burlingame, CA), and fluorescent microscopy was performed using an Olympus BX40 microscope equipped with Olympus UPlanF1 fluorescent optics. All images were acquired using the QCapture Suite software (version 2.60) and processed in Adobe Photoshop (version 7.0, San Jose, CA).

General methods and statistical analysis

Protein estimation was performed by Coomassie blue-dye binding assays as described (22), and 100 μg protein from each sample within an experimental group was resolved by SDS-PAGE for immunoblottings.

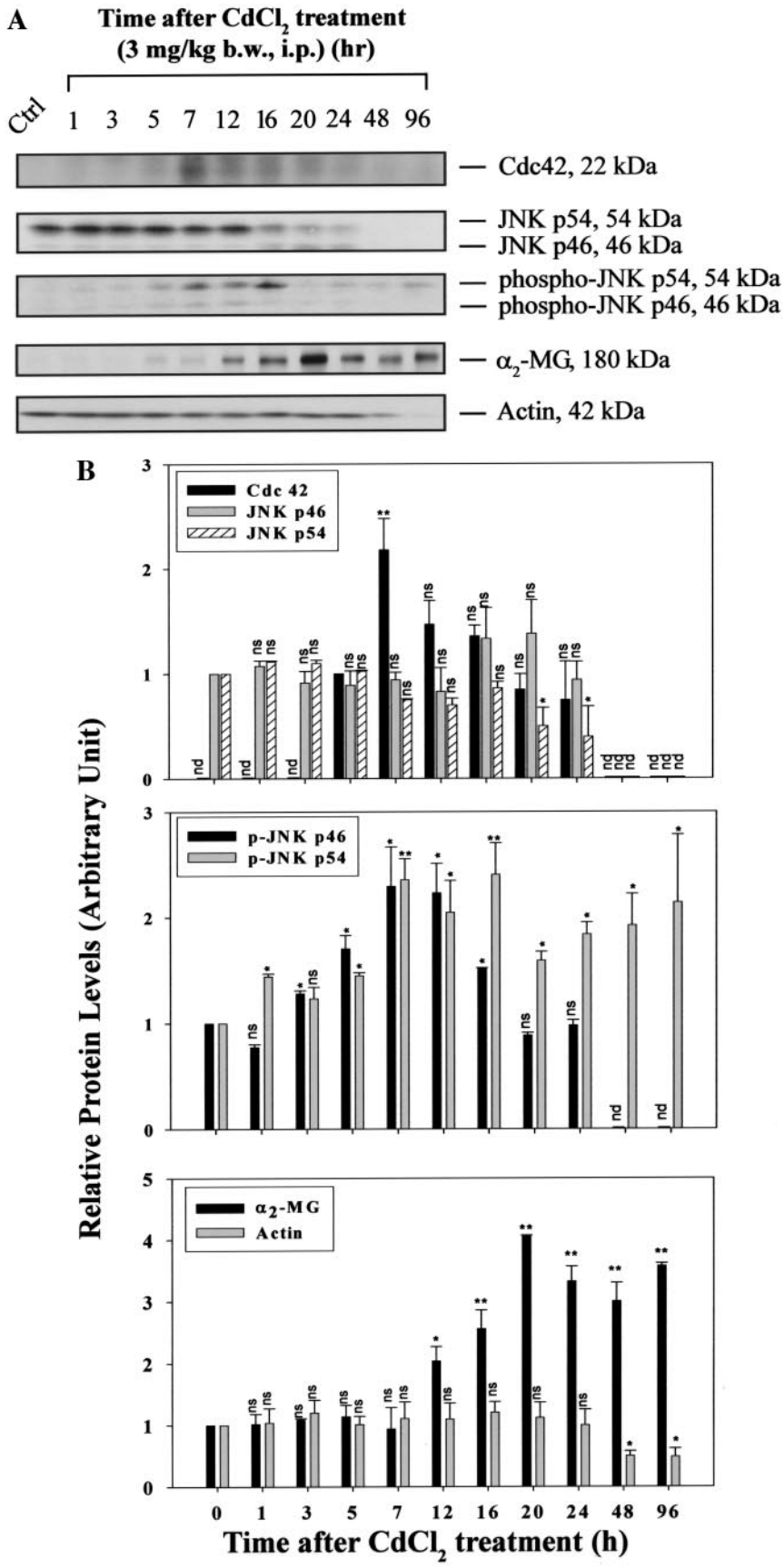

FIG. 1. Changes in the protein levels of Cdc42, JNK, phospho-JNK, α_2-MG, and actin in the testis during the $CdCl_2$-induced BTB damage in rat testes. A, Approximately 100 μg of protein from testis lysates of rats after $CdCl_2$ treatment (3 mg/kg body weight, ip) were resolved by SDS-PAGE using 7.5 or 12.5% T SDS-polyacrylamide gels. Immunoblot analyses were performed using different primary antibodies as indicated. All blots shown here were stripped and reprobed with an anti-β-actin antibody, as described in *Materials and Methods*, for loading controls as shown in the *bottom panel*. B, These are the corresponding densitometrically scanned results using immunoblots, such as those shown in A. Each *bar* is the mean ± SD of three to five determinations from three to five rats. The protein level of a target protein at time 0 was arbitrarily set at 1, against which one-way ANOVA was performed. nd, Nondetectable; ns, not significantly different by ANOVA. *, Significantly different by ANOVA, $P < 0.05$; **, significantly different by ANOVA, $P < 0.01$.

For results reported in Figs. 1 and 2, the blots that were striped and reprobed with an antiactin antibody were used to assess equal protein loading between samples within an experimental group. The intra- and interexperiment coefficients of variation based on at least 20 antiactin-stained immunoblots over a period of 12 wk were about 6 ± 2 and 10 ± 3%, respectively; and a decline in actin level was detected by 48 and 96 h after $CdCl_2$ treatment. As such, results of target proteins reported in Figs. 1 and 2 were not corrected for actin. However, for data reported elsewhere (see Figs. 3 and 7), changes in target proteins were also normalized against actin between samples, which had a coefficient of variation ranging between 3 and 6%. Statistical analyses were performed by ANOVA with Tukey's honestly significant difference tests or Student's *t* tests using the GB-STAT statistical analysis software package (version 7.0; Dynamic Microsystems, Silver Spring, MD).

Results

Induction of α_2-MG and signal transducers of the JNK pathway in testes during $CdCl_2$-induced BTB damage

During $CdCl_2$ (3 mg/kg body weight, ip)-induced BTB damage, the induction of α_2-MG, unlike cathepsin L, a protease that was also induced, was not regulated by TGFβ3 via the p38 MAPK pathway (6). Interestingly, it was noted that before the significant induction of α_2-MG at 12–96 h (Fig. 1, A and B), a transient induction of Cdc42, a putative upstream activator of JNK, was detected between 5 and 24 h after $CdCl_2$ treatment (Fig. 1, A and B). The levels of JNK p54 and p46 stayed relatively stable until 16 and 24 h, respectively, after the treatment (Fig. 1, A and B). Both JNKs were almost undetectable by 48 h when the epithelium was badly damaged and virtually devoid of all germ cells (see below). More important, the phosphorylated JNKs were also transiently induced by a staggering 3-fold between 5 and 16 h (Fig. 1, A and B). Collectively, these data illustrate that the JNK signaling pathway might have been activated and used to regulate α_2-MG level in the epithelium during $CdCl_2$-induced BTB disruption. The levels of actin in the testis samples were also quantified, which served as a control for equal protein loading between 0 and 24 h after the treatment (see Fig. 1A, *bottom panel*) because a significant decline in actin level was detected at 48–96 h after the $CdCl_2$ treatment, which is consistent with earlier reports illustrating that $CdCl_2$ exposure can induce fragmentation of actin microfilament bundles and reduce its protein level in the rat seminiferous epithelium (6, 18) (see Fig. 1, A and B).

Activation of the intrinsic JNK activity during $CdCl_2$-induced BTB damage

To further investigate whether the JNK signal transduction pathway is indeed activated during $CdCl_2$-induced BTB damage, a kinase assay was performed to quantify the intrinsic JNK activity in testes. In brief, JNK activity in protein lysates was measured based on its ability to phosphorylate c-Jun, a transcription factor that activated specifically by JNK. The results shown in Fig. 2 have clearly illustrated a remarkable induction in the intrinsic activity of JNK between 7 and 12 h after $CdCl_2$ treatment, consistent with the immunoblotting data that showed transiently induced protein

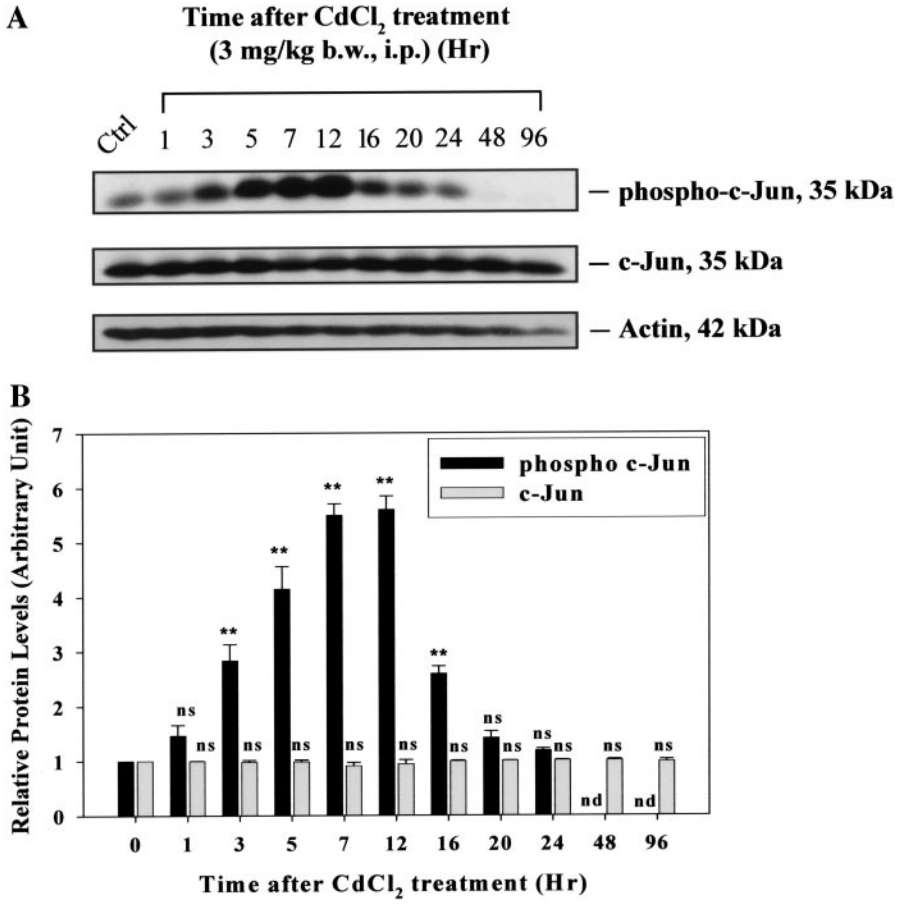

FIG. 2. Activation of JNK during $CdCl_2$-induced BTB damage. A, The level of activated JNK in the testis lysate after $CdCl_2$ treatment was evaluated using a pull-down kinase assay as described in *Materials and Methods*. Phosphorylation of c-Jun, which represents the intrinsic activity of JNK, was visualized by immunoblotting. The same blot was stripped and reprobed with a c-Jun antibody to ensure equal loading of c-Jun fusion protein. Also shown is the immunoblotting result using an antiactin antibody to illustrate equal protein loading in each reaction. B, This figure summarizes the densitometrically scanned result using immunoblots such as those shown in A. The assay was preformed three times using different sets of samples. Each *bar* is the mean ± SD of three separate experiments. The protein level of phospho-c-Jun and c-Jun at time 0 was arbitrarily set at 1, against which ANOVA was performed. nd, Nondetectable; ns, not significantly different by ANOVA. *, Significantly different by ANOVA, $P < 0.05$; **, significantly different by ANOVA, $P < 0.01$.

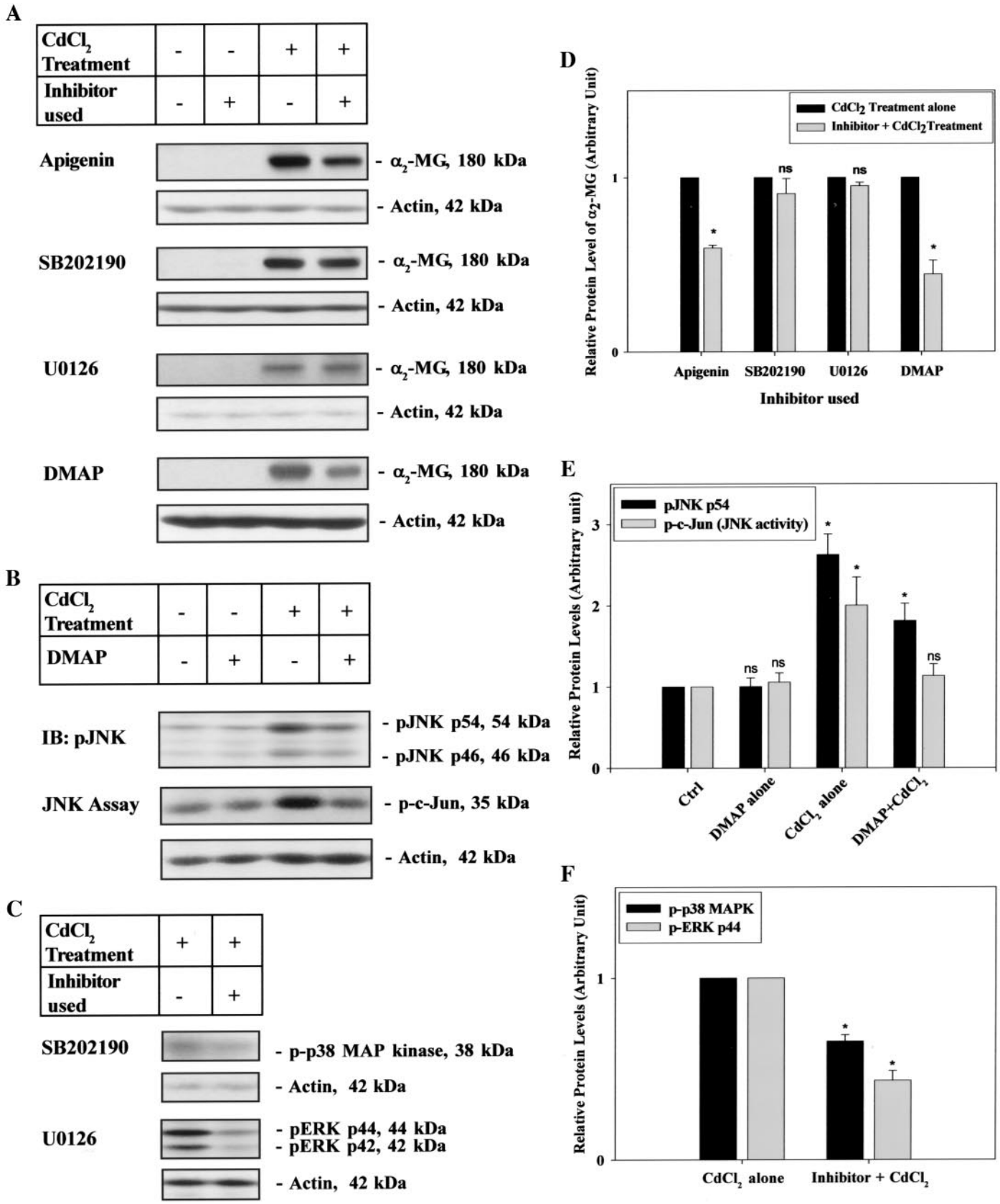

FIG. 3. Effects of different MAPK inhibitors on the level of $CdCl_2$-induced α_2-MG production in rat testes during the BTB damage. A, Normal rats and rats treated with $CdCl_2$ alone, MAPK inhibitor alone, or MAPK inhibitor + $CdCl_2$ were terminated at 16 h post treatment, and their

level of phospho-JNK (see Fig. 1). Note that the peak activity of JNK was achieved at 12 h after the treatment, which was slightly ahead of the time that the protein level of α_2-MG was the highest in immunoblot analysis (16 h after treatment, see Fig. 1). This slight delay is possible because after the activation of the JNK, a series of events, including transcription activation, gene expression, and protein modification, has to take place before an induction of protein level of α_2-MG could be detected. When the blots used in the assay were reprobed with an antibody against total c-Jun, there was no significant difference between samples, indicating equal loading of c-Jun fusion proteins (Fig. 2, A and B). Immunoblotting was also performed using an antiactin antibody to confirm equal protein loading between 0 and 24 h (Fig. 2A).

Effects of different MAPK inhibitors on the $CdCl_2$-induced α_2-MG production in the testis

To elucidate whether the JNK signaling pathway was indeed used to specifically regulate the production of α_2-MG during $CdCl_2$-induced BTB damage, a series of experiments was performed using different MAPK inhibitors. In this study, rats (n = 3) received an i.t. injection of a MAPK inhibitor (see Table 1) at three sites per testis, to be followed by a single dose of $CdCl_2$ (3 mg/kg body weight, ip). Normal rats, rats receiving inhibitor or $CdCl_2$ alone, served as controls. In each treatment group, rats were killed by 16 h, and testis lysates were analyzed by immunoblotting using an anti-α_2-MG antibody (Fig. 3A). It was shown that apigenin, an inhibitor for all MAPKs (23), was able to significantly reduce the $CdCl_2$-induced α_2-MG surge (Fig. 3, A and D). This result clearly indicates that the expression of α_2-MG during the $CdCl_2$-induced BTB damage was regulated via a MAPK pathway. However, the use of SB202190, a specific p38 MAPK inhibitor (24), and U0126, a specific MEK/ERK 1/2 inhibitor (25), did not result in a lowering of the α_2-MG production during $CdCl_2$-induced BTB damage. These findings suggest that neither p38 MAPK nor ERK plays a role in regulating α_2-MG during $CdCl_2$-induced BTB damage. Yet DMAP, an inhibitor that was shown to block specifically the activation of JNK in mouse Sertoli cells (26), significantly reduced the $CdCl_2$-induced α_2-MG surge in the testis, similar to the effects of apigenin (Fig. 3, A and D).

To further verify whether DMAP indeed blocked the intrinsic JNK activity in the testis, samples were subjected to an intrinsic kinase assay (Fig. 3, B, *middle panel*, and E) as well as the quantification of p-JNK (Fig. 3, B and E). Although DMAP *per se* had no apparent effect on the basal p-JNK protein level and its basal intrinsic kinase activity, it could effectively block the $CdCl_2$-induced intrinsic JNK activity and lower the $CdCl_2$-induced p-JNK level (Fig. 3, B and E). These data thus illustrate that DMAP indeed functions as a JNK inhibitor *in vivo*. The inhibitory effects of SB202190 and U0126 on p38 MAPK and ERK, respectively, were also assessed by immunoblotting using phospho-specific antibodies against the corresponding MAPK (Fig. 3, C and F). The phosphorylated forms of the both p38 and ERK were markedly reduced when testes were pretreated with the corresponding inhibitor before $CdCl_2$ administration, compared with $CdCl_2$ alone, suggesting that the activities of these kinases were indeed inhibited, even though the α_2-MG level was not affected apparently (Fig. 3, C and F, *vs.* Fig. 3, A and D). These findings thus have unequivocally demonstrated that the $CdCl_2$-induced α_2-MG production in the testis is mediated via the JNK signaling pathway but neither the p38 MAPK nor the ERK pathways.

The use of DMAP worsens the kinetics of germ cell loss from the seminiferous epithelium during $CdCl_2$-induced BTB damage

To assess the functional significance of α_2-MG induction during $CdCl_2$-induced BTB restructuring, we investigated whether DMAP pretreatment can worsen the kinetics of germ cell loss from the epithelium during $CdCl_2$ treatment when α_2-MG production was suppressed. In rats receiving $CdCl_2$ alone, the morphology of the seminiferous epithelium was indistinguishable from normal testes during the first 10 h after $CdCl_2$ treatment (Fig. 4, A–C). Thereafter, germ cells were shown to dislodge from the epithelium, emptying into the lumen prematurely (Fig. 4, E and G), indicating that the apical ES was disrupted at the time the BTB was damaged (see below). However, when rats were pretreated with DMAP before $CdCl_2$ administration to block the production of α_2-MG in the epithelium, germ cells were found in the lumen as early as 10 h after DMAP+$CdCl_2$ treatment in at least 10% of the tubules scored (Fig. 4, D *vs.* C). At 14 h, more tubules appeared abnormal with germ cells found in the tubule lumen (Fig. 4, F *vs.* E). Nonetheless, whereas DMAP worsened the damage of $CdCl_2$ to the testis by disrupting Sertoli-germ cell adhesion, the integrity of the microvascular TJ barrier was not compromised (Fig. 4, D and F, *vs.* Fig. 4, C and E). At approximately 20 h after the treatment, most tubules had epithelium with patches of voided areas, and red blood cells were found in the interstitium because the endothelial barrier of blood capillaries was damaged by $CdCl_2$ (Fig. 4H). To better illustrate the difference between the two treatment groups, percentages of tubules with normal distribution of germ cells in each testis at each time point were scored (Fig. 4I). In rats pretreated with DMAP to block α_2-MG production by inhibiting JNK activity, such a decline in α_2-MG level indeed increased the percentage of abnormal tubules with premature germ cell loss *vs.* $CdCl_2$ treatment alone (Fig. 4I).

testis lysate was analyzed by immunoblotting using an anti-α_2-MG antibody. B, Effect of DMAP on the inhibition of intrinsic JNK activity was validated by immunoblotting using a phospho-specific JNK antibody and a JNK intrinsic activity assay. C, Inhibitions of p38 MAPK by SB202190 and ERK by U0126 during $CdCl_2$-induced BTB damage were validated by immunoblotting using anti-phospho-p38 and anti-p-ERK antibodies. The blots shown in A–C were subsequently stripped and reprobed with an antiactin antibody to confirm equal protein loading. D–F, These are the corresponding densitometrically scanned results using immunoblots, such as those shown in A–C, respectively. D, The protein level of α_2-MG in rats treated with $CdCl_2$ alone was arbitrarily set at 1, against which Student's *t* test was performed. Each *bar* in D–F is the mean ± SD of three to four determinations from three to four rats and normalized against actin. ns, Not significantly different by *t* test. *, Significantly different by *t* test, $P < 0.05$.

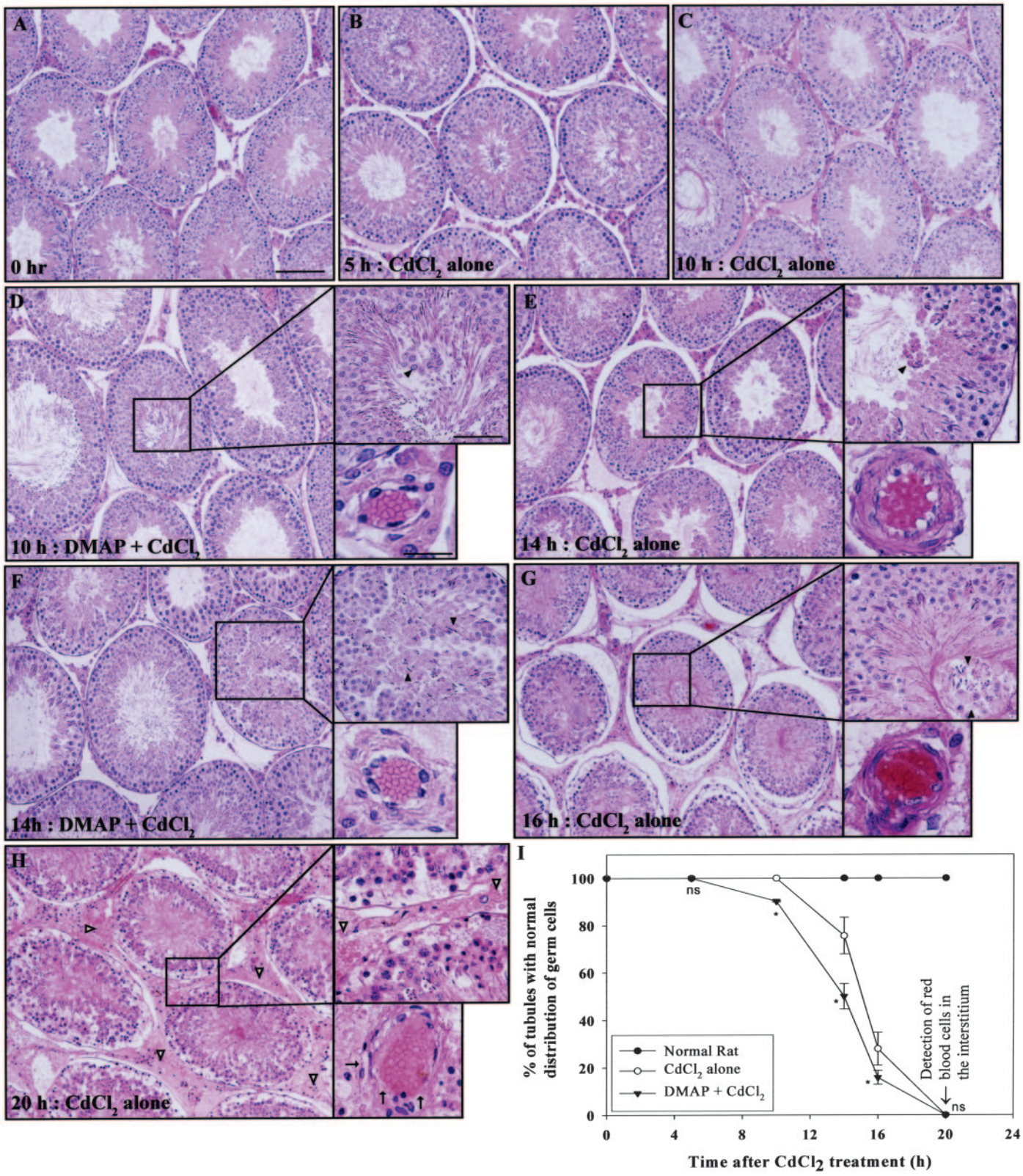

FIG. 4. A study to assess the kinetics of germ cell loss from the epithelium and the occurrence of the microvascular TJ barrier disruption after $CdCl_2$ treatment or DMAP plus $CdCl_2$ treatment. A–F, These are micrographs of paraffin-embedded sections of testes stained by hematoxylin-eosin from normal rats (A), rats receiving $CdCl_2$ at 3 mg/kg body weight alone (B, C, E, G, and H), and rats receiving DMAP pretreatment (8 μmol/testis) + $CdCl_2$ (D and F). Rats were terminated at the specified time points. Germ cells were sloughed to the lumen after $CdCl_2$-induced BTB damage (*black arrowheads*), which were not found in normal rat testes (see A). Red blood cells were found in the interstitium 20 h after

To further assess the ultrastructural changes in the testis after treatment of rats with DMAP and/or $CdCl_2$, electron microscopy was used to examine testes from normal rats (Fig. 5A) or rats receiving the treatments for 10 or 20 h (Fig. 5). In normal rat testes, the BTB, which is composed of TJs and basal ES, which was identified as the hexagonally packed actin filaments sandwiched between the cisternae of ectoplasmic reticulum (er) and Sertoli cell membrane, such as those shown in Fig. 5, A and B, was clearly visible in the seminiferous epithelium (Fig. 5, A–C). Apical ES, which structure was virtually identical to that of the basal ES but was confined only to the Sertoli cell, is shown in Fig. 5D. The microvessel found in the interstitium of a normal rat is shown in Fig. 5, E and F, with the endothelial cells forming a tight endothelium surrounding the blood vessel. However, when rats were treated with $CdCl_2$ for 10 h (3 mg/kg body weight, ip), it was noticed that TJs at the BTB began to be disrupted because intercellular space could be observed between two adjacent Sertoli cell membranes in some sections (Fig. 5, G and H). At the site of disruption in the BTB, the cisternae of endoplasmic reticulum and the associated actin bundles in the basal ES were lost (Fig. 5H). BTB disruption was even more extensive and readily observable in rats treated with DMAP+$CdCl_2$ for 10 h (Fig. 5, I and J), illustrating that DMAP had indeed worsened the BTB damage. The actin bundles at the basal ES had become disintegrated and were less extensive *vs.* control in which they were still present (Fig 5, I and J, *vs.* Fig. 5, B and C), which was consistent with a previous report that actin was disrupted by a single low doe of $CdCl_2$ (18). The apical ES was also affected by the DMAP+$CdCl_2$ treatment at 10 h, which was possibly the reason for germ cell loss at this time point (Fig. 5K). Microvessel damage in rat testes was seen only at 20 h after $CdCl_2$ treatment (Fig. 5L), in which extensive damage was found at the endothelium of the microvessel with obvious gaps between cells.

Pretreatment of rats with DMAP reduces the $CdCl_2$-induced production of α_2-MG in the seminiferous epithelium

In normal rat testis, α_2-MG was confined mainly to the perinuclear region of Sertoli cells and around the heads of elongating and elongated spermatids at the site of apical ES in stages XI–VII, and was also in the interstitium associated with blood vessels and possibly Leydig cells (Fig. 6A). However, the intensity of immunoreactive α_2-MG in the basal compartment of the seminiferous epithelium, consistent with its localization at the site of the BTB, increased significantly by 16 h after $CdCl_2$ treatment (Fig. 6, D *vs.* A). Furthermore, α_2-MG was localized to the heads of developing spermatids that were being sloughed to the tubule lumen (Fig. 6D). Treatment of testes with DMAP alone affected neither the histology nor localization of α_2-MG in the seminiferous epithelium (Fig. 6C *vs.* 6, A and B). However, in rats treated with DMAP+$CdCl_2$, the staining of α_2-MG at the cell-cell interface in the seminiferous epithelium was markedly reduced when compared with the rat that received $CdCl_2$ treatment alone (Fig. 6, E *vs.* D), consistent with the results of immunoblotting (see Fig. 3). Moreover, when the α_2-MG level was reduced by DMAP treatment in the testis, it augmented the $CdCl_2$-induced damage in the epithelium with more patches of voided areas *vs.* $CdCl_2$ treatment alone due to an increase in the germ cell loss (Fig. 6, E *vs.* D; see also Fig. 4I), suggesting that the BTB and the seminiferous epithelium was damaged more extensively. In control sections using normal rabbit serum in substitution of α_2-MG antiserum (Fig. 6B), no detectable staining was observed in the epithelium, indicating the specificity of the α_2-MG staining shown in Fig. 6, A and C–E. Other controls including replacing the primary antibody with PBS and using normal goat serum instead of the secondary antibody yielded no detectable staining (data not shown).

Effects of DMAP pretreatment on the levels of TJ- and AJ-associated proteins in the testis and the status of BTB and anchoring junctions

To evaluate the effects of DMAP pretreatment to $CdCl_2$-induced damage to TJs and AJs, immunoblotting and immunofluorescent microscopy were performed to examine the levels of several TJ and AJ constituent proteins, using testes from normal rats, rats treated with either DMAP or $CdCl_2$ alone, and rats receiving DMAP+$CdCl_2$ treatment (Figs. 7–9). When comparing normal testes with testes administrated with DMAP alone, the protein levels of occludin, ZO-1, N-cadherin, E-cadherin, and β-catenin did not significantly change (Fig. 7, A and B). After $CdCl_2$ treatment, the levels of these proteins in the testis were significantly reduced (Fig. 7, A and B), consistent with an earlier report (6). However, there was a more pronounced and significant reduction in the levels of TJ- and AJ-associated proteins in testes with DMAP+$CdCl_2$ treatment when compared with testes receiving treatment of $CdCl_2$ alone (Fig. 7, B and C), illustrating that the epithelium had sustained more $CdCl_2$-induced damage because of a loss of α_2-MG. The immunoblotting result was further supported by immunofluorescent studies colocalizing occludin with ZO-1 (Fig. 8), and N-cadherin with β-catenin (Fig. 9), in the seminiferous epithelium. In normal testes or testes treated with DMAP alone, the staining of occludin/ZO-1 (Fig. 8, E–H) and N-cadherin/β-catenin (Fig. 9, D–F) was found at the BTB site near the basement membrane, indistinguishable from control (normal) rat testes (Fig. 8, A–D, *vs.* Fig. 8, E–H and Fig. 9, A–C, *vs.* Fig. 9, D–F). The fluorescent stainings were greatly re-

treatment (H, *white arrowheads*) when the endothelial barriers of blood vessels were damaged (as indicated by *arrows*). I, The composite result of this study that illustrates the kinetics of germ cell loss from the seminiferous epithelium by comparing the percentage of tubules with normal germ cell distribution in rat testes of the two treatment groups at different time points. About 200 cross-sections from three rat testes for each treatment at each time point were analyzed, and the number of normal *vs.* damaged tubules was tallied (see *Materials and Methods*). *Bar* (A), 80 μm, which applies to B–H. *Bar* (D, *large inset*), 40 μm, which applies to the corresponding insets in E–H. *Bar* (D, *small inset*), 20 μm, which applies to the corresponding insets in E–H. Statistics were performed by *t* test, comparing the DMAP pretreatment group with $CdCl_2$ alone to assess the effects of DMAP in worsening the epithelial damage in the testis. ns, Not significantly different from rats receiving $CdCl_2$ alone at the corresponding time point. *, Significantly different by *t* test, $P < 0.05$.

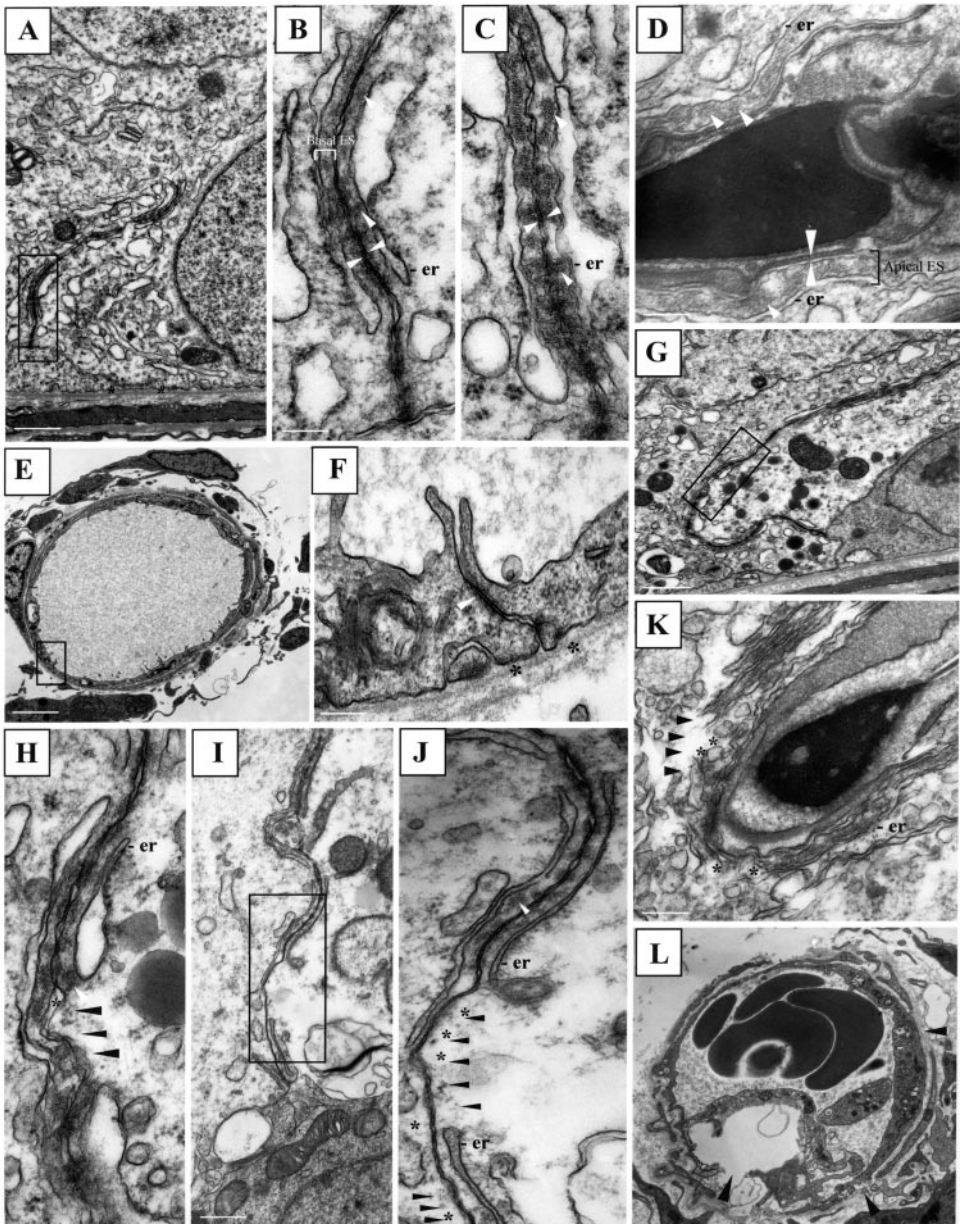

FIG. 5. A study using electron microscopy to assess ultrastructural changes in the testis after treatment of rats with $CdCl_2$. A–F, Electron micrographs of normal rat testes. A, Cross-section of an ST showing the seminiferous epithelium lying on the basement membrane (*asterisks*). The *boxed region* represents the BTB between two Sertoli cells. B, Magnified view of the BTB shown in A, which is composed of TJs and the basal ES between two apposing Sertoli cell membranes (*opposing white arrowheads*). Hexagonally packed actin (*white arrowheads*) was found between cisternae of er and Sertoli cell membrane, which is the typical structure of ES. C, Another highly magnified area in a normal adult rat testis, showing the BTB, which was composed of TJs and basal ES. D, The apical ES at the interface between the head of an elongating spermatid and Sertoli cell, which was found only on the Sertoli cell side. E, Microvessel located in the interstitium. The *boxed area* is shown in F. F, The endothelial cells were forming a tight endothelium surrounding the blood vessel with the typical TJs confined to the apical portion of cells (*white arrowhead*). The basal region of cells was in contact with the basal lamina (*asterisks*). G, Cross-section of a tubule from rats treated with $CdCl_2$ (3 mg/kg body weight, ip) for 10 h. The *boxed area* is the BTB. H, Magnified view of the BTB shown in G, in which TJs began to open up with space between two adjacent Sertoli cell membranes (*asterisk*). Also noted is the obvious absence of er and the associated actin bundles in the basal ES (*black arrowheads*). I, Cross-section of a tubule from rats treated with DMAP+$CdCl_2$ for 10 h. The BTB displayed more extensive damage *vs.* $CdCl_2$ alone. J, In this magnified view of the BTB shown in I, it is apparent that the actin bundles at the basal ES had become disorganized (*asterisks*), whereas some were still being detected (*white arrowhead*), they were less extensive *vs.* control (see B and C) and even rats subjected to $CdCl_2$ only (see H). Actin bundles (*asterisks*) and er (*black arrowheads*) were also absent. K, Dissolution of the apical ES with the loss of actin bundles (*asterisks*) and er (*black arrowheads*) from the apical ES. L, Typical microvessel from rats after 20 h of $CdCl_2$ treatment, showing extensive damage to the endothelium with obvious gaps between endothelial cells (*black arrowheads*). Bar (A), 2.5 μm; B, 0.6 μm, which applies to C, H, and J; D, 0.5 μm; E, 5 μm, which applies to L; F, 0.4 μm; G, 3 μm; I, 2 μm; K, 0.75 μm.

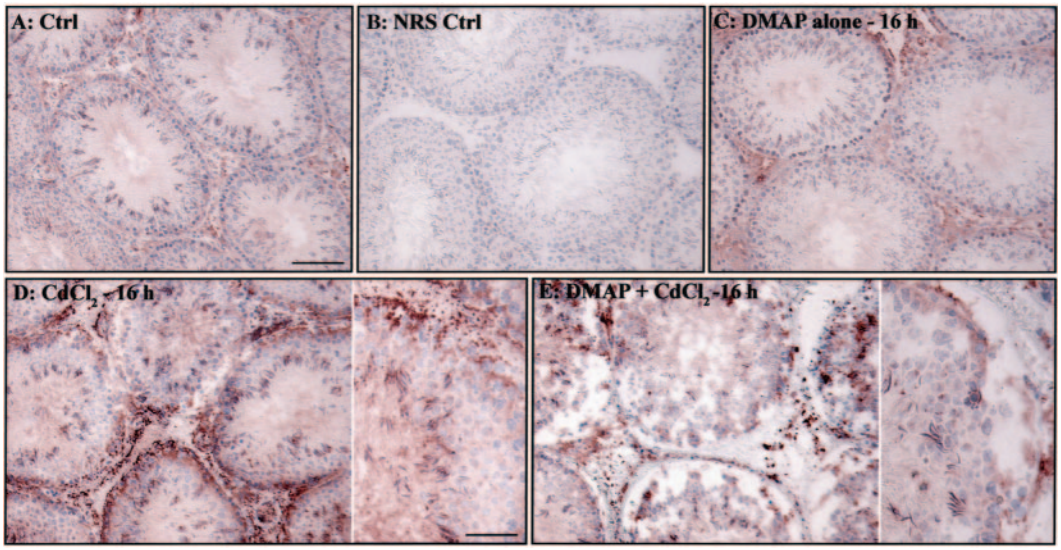

FIG. 6. Effects of DMAP pretreatment on the cell localization of α_2-MG in the seminiferous epithelium during $CdCl_2$-induced BTB damage. A, Immunohistochemistry was performed to localize α_2-MG in the seminiferous epithelium of a normal rat testis. B, Control section substituting the anti-α_2-MG antiserum with preimmune normal rabbit serum (NRS) at the same dilution, which illustrates the specificity of the α_2-MG staining. C–E, The localization of α_2-MG in the seminiferous epithelium after the administration of DMAP alone (8 μmol, i.t.), $CdCl_2$ (3 mg/kg body weight, ip) alone (with 200 μl saline injected via i.t. as a vehicle control), and DMAP followed by $CdCl_2$, respectively. All samples were collected 16 h after the specified treatments. D and E (*right panels*), Higher magnification of a tubule such as those shown in the corresponding *left panels*. *Bar* (A), 80 μm, which applies to B–E. *Bar* (D, *right panel*), 40 μm, which applies to E (*right panels*).

duced by $CdCl_2$ *per se* at 16 h after treatment, but the intensity was even further reduced to an almost nondetectable level in the DMAP+$CdCl_2$ treatment group (Figs. 8, I–P, and 9, G–L). Collectively these results further confirm the notion that both TJs and AJs in the seminiferous epithelium were more severely damaged by $CdCl_2$ when the level of α_2-MG was suppressed by blocking the JNK signaling pathway. These results thus provide an unequivocal proof regarding the crucial role of protease inhibitors in BTB dynamics.

Discussion

The production of α_2-MG by Sertoli cells in the seminiferous epithelium is regulated via the JNK signaling pathway

α_2-MG is an acute-phase protein that can be induced by more than 100-fold in the systemic circulation during inflammation (27, 28). In mammalian cells, such as hepatocytes and neuronal cells, the secretion of this protease inhibitor is regulated by inflammatory cytokines, such as IL-6 (29, 30). Furthermore, α_2-MG can be stimulated by other cytokines, such as TGFβ and interferon-γ, in adrenocortical and astrocytoma cells (31, 32). Yet α_2-MG secretion by Sertoli cells is not regulated by IL-6 at doses that are known to stimulate its secretion by hepatocytes (33). Other studies have also shown that α_2-MG is not an acute-phase protein in the testis, and it is responsive to neither cytokines nor glucocorticoids that are known regulators of α_2-MG in the liver. Interestingly, its level has to be maintained at relatively high level in the testis, which is likely to be used for protecting the epithelium during tissue restructuring pertinent to spermatogenesis (34–36). In a previous report using $CdCl_2$-induced TJ disruption as a model to investigate BTB dynamics, the level of α_2-MG in the testis, in particular at the site of BTB, was shown to be induced by $CdCl_2$ (1 or 3 mg/kg body weight, ip) (6). Yet the signaling pathway(s) that regulates α_2-MG is virtually unknown because the use of SB202190, which blocked p38 MAPK activity, had no effect on the level of α_2-MG in the epithelium, even though it could rescue the loss of occludin and ZO-1 from the TJ site as well as the cadherin-catenin and the nectin-afadin complexes from the AJ site (6).

MAPKs, such as p38 MAPK and JNK, have recently been shown to be crucial signal transducers that regulate TJ dynamics (for reviews, see Refs. 37, 38). To investigate whether α_2-MG is also regulated by this class of molecules, experiments were performed in which different MAPK inhibitors were administered i.t. before $CdCl_2$ treatment to assess the steady-state levels of α_2-MG in testes during BTB damage. Indeed, apigenin, a general inhibitor of MAPKs, significantly reduced the induction of α_2-MG by $CdCl_2$. When all three MAPKs, namely ERK, p38, and JNK, were examined by using their corresponding specific inhibitors, only DMAP resulted in a significant reduction in the $CdCl_2$-induced α_2-MG production by testes similar to that caused by apigenin. DMAP was also shown in an earlier study that could specifically block the TNFα-induced JNK activation in mouse Sertoli cells (26, 39) and human fat cells (40). Although in one study DMAP was also shown to inhibit p38 MAPK phosphorylation, the possibility that α_2-MG was regulated via the p38 MAPK pathway has been ruled out (26). This is supported by the result from the present study that SB202190, a specific p38 inhibitor, failed to affect the $CdCl_2$-induced α_2-MG production. Collectively these findings strongly favor the notion that the α_2-MG induction that occurs during BTB disruption is regulated via the JNK pathway. We speculate that this activation of JNK and the subsequent induction of α_2-MG production in the seminiferous epithelium are stimulated by cytokines, such as TGFβ and TNFα, which are the

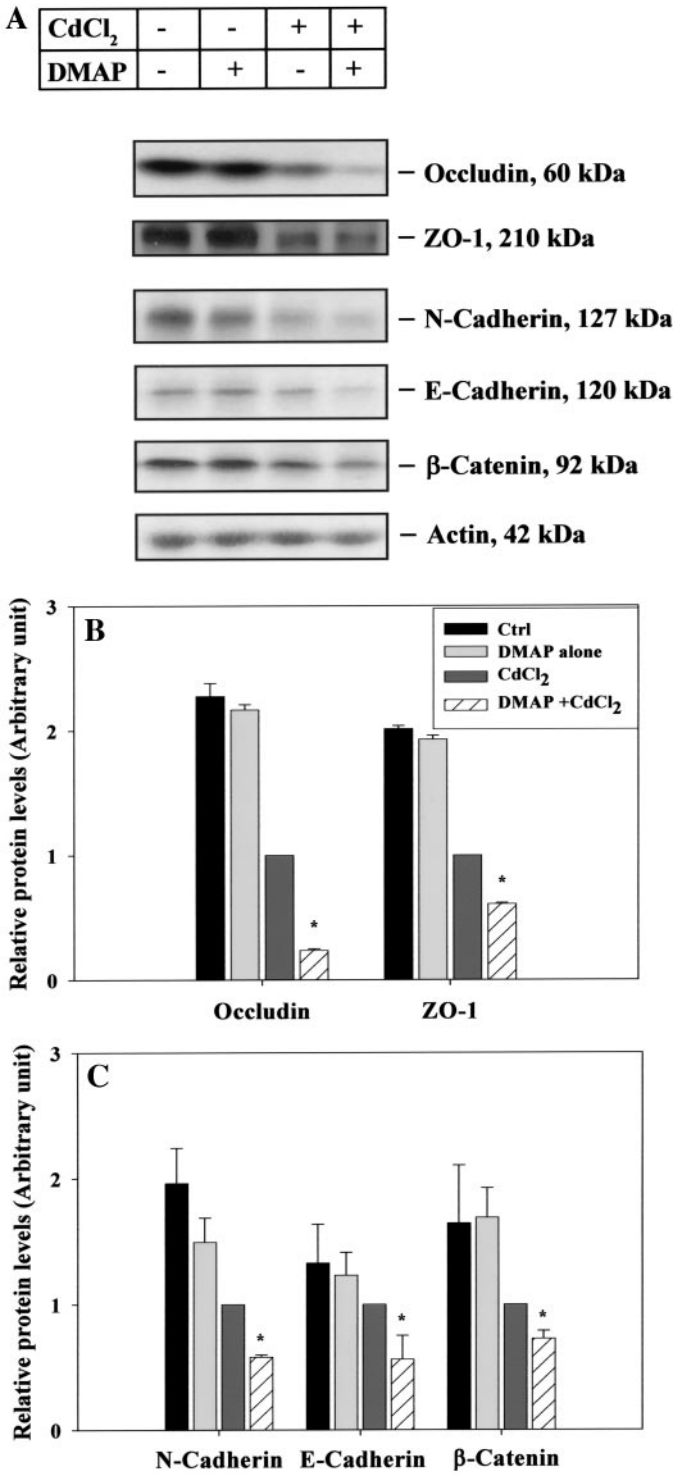

FIG. 7. A study to assess the mechanism by which DMAP worsens the $CdCl_2$-induced damage to the seminiferous epithelium. Effects of DMAP on the expression of TJ and AJ proteins in the epithelium during $CdCl_2$-induced BTB damage were assessed by immunoblottings, which monitor the levels of TJ-and AJ-associated proteins found at the BTB. A, The effect of DMAP pretreatment + $CdCl_2$ on junction proteins *vs.* DMAP alone, $CdCl_2$ alone, and normal rats. Testes were collected 16 h after each treatment, and lysates were analyzed using different antibodies as specified. Immunoblot using an antiactin antibody was shown in the *lower panel* to indicate relatively equal protein loading. B and C, Two histograms that show the corresponding densitometrically scanned result using immunoblots such as those shown in A. Each *bar* is the mean ± SD of results of three to four rats. The protein levels of target proteins in testis lysates from rats receiving $CdCl_2$ was arbitrarily set at 1. Student's *t* test was performed to compare data between DMAP+$CdCl_2$ and $CdCl_2$ alone. ns, Not significantly different by *t* test. *, Significantly different by *t* test, $P < 0.05$.

known upstream activators of the MAPK pathways and are also products of Sertoli and germ cells, such as spermatocytes and spermatids (for reviews, see Refs. 37 and 41). It is likely that cytokines produced by preleptotene and leptotene spermatocytes in the rat testis regulate the physiological function of Sertoli cells including BTB restructuring to permit their passage through the Sertoli cell TJ barrier at late-stage VIII through early-stage IX of the epithelial cycle in the rat testis (for a review, see Ref. 42).

α_2-MG, regulated via the JNK pathway, is necessary for the maintenance of the BTB

In the present study, DMAP was shown to down-regulate α_2-MG protein level in the seminiferous epithelium during $CdCl_2$-induced BTB disruption, worsening the extent of damage to the epithelium, possibly because of the unchecked proteolysis. This conclusion was reached based on the following observations. First, morphological studies have revealed a significantly different profile of kinetics of germ cell loss from the epithelium after $CdCl_2$ administration between rats with and without DMAP pretreatment. In rats treated with $CdCl_2$ alone, germ cells did not start being emptied to the tubule lumen until approximately 14 h, but tubules with immature germ cells in the lumen were detected as early as approximately 10 h after DMAP+$CdCl_2$ treatment. This loss of germ cell induced by $CdCl_2$ occurred somewhat later than the disruption of TJs at the BTB, which was reported to occur approximately 7 h after $CdCl_2$ administration (6), indicating that Sertoli-germ cell AJ disruption is indeed secondary to BTB damage. Furthermore, even though the epithelium was badly damaged in more than 90% of the tubules in rats treated with $CdCl_2$ alone, the damage found in the epithelium from rats with DMAP pretreatment before $CdCl_2$ administration was more extensive (see Fig. 6). In more than 80% of tubules examined, the entire epithelium was shredding from the basement membrane (see Fig. 6, E *vs.* D). As such the kinetic data shown in Fig. 4I are an underestimation on the worsening effects of DMAP to the epithelium because the extent of the damage as illustrated in Fig. 6 was not taken into consideration.

The kinetics of germ cell loss observed in the light microscopic level were further supported by the ultrastructural analysis using electron microscopy, which showed that damages of the BTB and apical ES were indeed more extensive in testes receiving DMAP pretreatment. It was apparent that DMAP mediated its effects, at least in part, via a disruption of the actin filament network by disintegrating actin from the basal ES and apical ES sites. Additionally, it was noted that in both treatment groups, red blood cells leaking to the interstitium from the microvessels, and the disruption of the endothelium of microvessels were detected only at and after 20 h of $CdCl_2$ treatment. These were the results of vascular

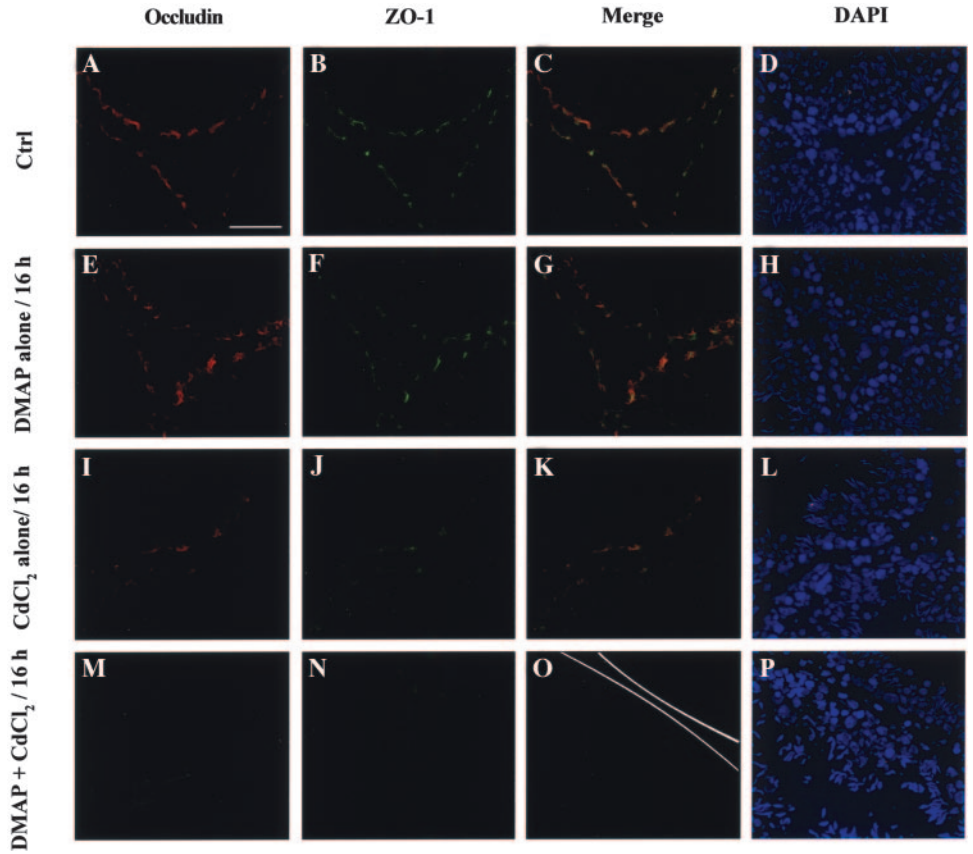

FIG. 8. A study to assess the BTB integrity by fluorescent microscopy, colocalizing occludin and ZO-1 in the seminiferous epithelium during $CdCl_2$-induced BTB damage with and without DMAP pretreatment. A–P, Immunofluorescent micrographs using cross-sections of normal rat testes (A–D), rat testes receiving only DMAP treatment (E–H), testes from rats that had been treated with $CdCl_2$ (I–L), and rat testes with DMAP pretreatment + $CdCl_2$ (M–P). Rats were killed at 16 h in all treatment groups. Occludin appeared as *red* fluorescence (Cy-3), whereas ZO-1 as *green* fluorescence (FITC). C, G, K, and O, Merged images of the corresponding immunofluorescent micrographs, in which occludin and ZO-1 colocalized as *orange* fluorescence. D, H, L, and P, The 4′,6′-diamino-2-phenylindole staining of the corresponding cross-sections that indicates the relative location of germ cells in the seminiferous epithelium. *White lines* (O) represent the relative location of the basement membrane of the seminiferous epithelium. *Bar* (A), 80 μm, which applies to B–P.

damage caused by $CdCl_2$ (17, 18), which took place only after BTB disruption, supporting the notion that the changes seen in seminiferous epithelium as reported herein are not secondary to anoxia and that the BTB is more susceptible to cadmium toxicity than TJs at the microvascular endothelium.

Second, the production of junction-associated proteins was more seriously affected by DMAP pretreatment. For instance, the protein levels of occludin (a TJ-integral membrane protein), ZO-1 (a TJ adaptor protein), N-cadherin, E-cadherin (two ES-associated integral membrane proteins), and β-catenin (an AJ adaptor) were significantly reduced when compared with the $CdCl_2$ treatment alone, as detected in both immunoblot analysis and immunofluorescent microscopy. This loss of proteins from the BTB and AJ (*e.g.* basal ES) was likely the result of a reduction in α_2-MG at these sites. Previous study has shown that different classes of proteases, including cathepsin L and matrix metalloprotease (MMP)-2, and another protease inhibitor, namely cystatin C, were induced in the testis during the $CdCl_2$-induced BTB disruption (6). When the balance between these proteases and protease inhibitors at the cell-cell interface in the epithelium was disturbed, such as in this case by blocking the production of α_2-MG via the effect of DMAP, excessive proteolysis and cleavage of junction proteins would take place, leading to the dissociation of junction complexes and the disruption of the BTB (Fig. 10). Obviously, this hypothesis must be rigorously tested in future studies including a quantification on the overall metallo-, serine-, histidine-, aspartate-, and/or cysteine-protease activities as well as their corresponding antiprotease activities during $CdCl_2$-induced damage with and without specific inhibitors.

Another possible role of α_2-MG in regulating junction dynamics in the epithelium is its ability to bind to cytokines, such as TGFβ (for a review, see Ref. 13), which were also known to induce junction disassembly in the testis (for reviews, see Refs. 37 and 43). Indeed, TGFβ3 was shown to bind to α_2-MG in the testis (6). As such, α_2-MG can also regulate junction dynamics in the epithelium by maintaining the level of cytokines via its interactions with these biological factors (Fig. 10). However, it is noteworthy that α_2-MG null mice are fertile and can produce litters of normal size and sex ratio (44, 45), suggesting that the presence of α_2-MG is not an absolute necessity for maintaining spermatogenesis or its loss can at least be superseded by another protease inhibitor(s) in the seminiferous epithelium. Nonetheless, this seemingly negative physiological finding does not rule out the significance of this molecule as reported

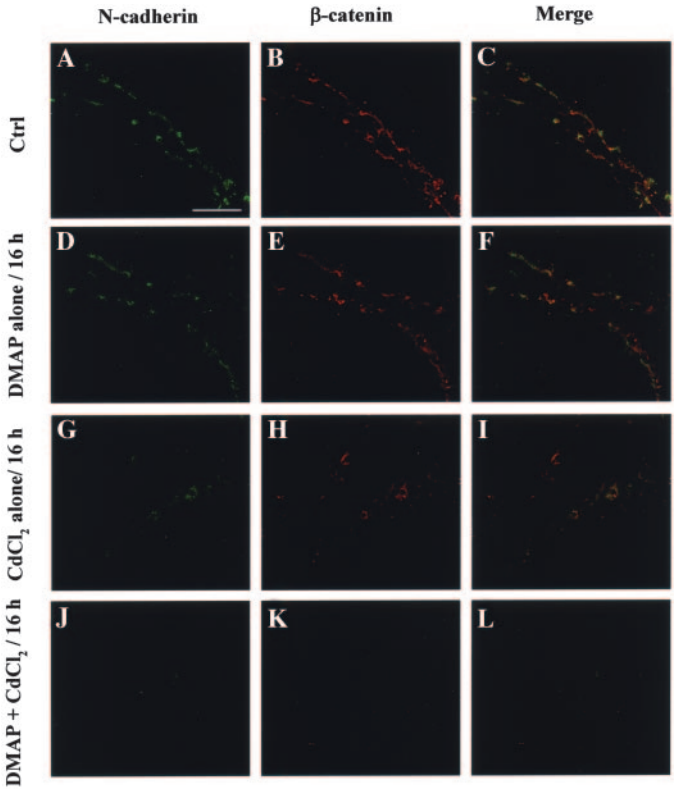

FIG. 9. A study to assess basal ES integrity at the BTB site by fluorescent microscopy, colocalizing N-cadherin and β-catenin in the seminiferous epithelium during $CdCl_2$-induced BTB damage with and without DMAP pretreatment. A–P, Immunofluorescent staining of N-cadherin (*green*, FITC), β-catenin (*red*, Cy-3), and the corresponding merged images of testes cross-sections from normal rat testes (A–C), rat receiving only DMAP treatment (D–F), $CdCl_2$ treatment (G–I), and DMAP pretreatment + $CdCl_2$ (J–L). All rats were killed 16 h post treatment, which was shown to display extensive BTB damage (see Fig. 4). The colocalized N-cadherin and β-catenin, which appeared as *orange* fluorescence, were found at the basal compartment adjacent to the basement membrane consistent with their localization at the BTB site. *Bar* (A), 20 μm, which applies to B–L.

herein. Due to the complexity of spermatogenesis and its significance to maintain the perpetuation of a species, it is highly likely that several regulatory pathways or different molecules are working in concert to accommodate a specific function to ensure the normal functioning of the seminiferous epithelium. Thus, the knockout of α_2-MG in mice may be compensated by another protein(s) with a similar role to maintain fertility. Although α_2-MG deficiency did not affect normal spermatogenesis as shown in the α_2-$MG^{-/-}$ mice, it may well be crucial to protect the seminiferous epithelium when the testis is under assault from environmental stress, such as cadmium toxicity in this case. In fact, this possibility was strengthened by the observation that α_2-$MG^{-/-}$ mice were highly susceptible to diet-induced pancreatitis, even though the knockout *per se* did not affect vitality (45).

The fact that α_2-MG plays a critical role in the maintenance of the BTB integrity, as shown herein, is physiologically significant because it provides yet another proof that proteolysis is involved in regulating junction dynamics at the cell-cell interface in the seminiferous epithelium, unlike other epithelia in which proteolysis is restricted to the cell-matrix anchoring junctions (for review, see Refs. 1, 2, 46, and 47). Recent studies have also shown that MMP-2, membrane type 1-MMP and tissue inhibitor of metalloprotease-2 in the rat testis colocalize with β1-integrin and laminin γ3 at the apical ES (48). More important, the use of specific inhibitors of MMPs can indeed worsen the damage to the seminiferous epithelium by 1-(2,4-dichlorobenzyl)-indazole-carbohydrazide, a reagent known to perturb cell adhesion function in the testis (48). An earlier study monitoring the levels of total cysteine and serine proteases during Sertoli-germ cell AJ assembly also illustrated an induction of protease activities, which was followed by an increase in α_2-MG and cystatin C (a specific cysteine protease inhibitor) steady-state mRNA levels (10). These earlier results coupled with the data presented herein have proven beyond refute regarding the significance of proteolysis in cell-cell junction restructuring in the testis. They also strengthen the concept that AJs (and possibly TJs) in the testis are hybrid junction types that have the properties and characteristics of cell-cell and cell-matrix anchoring junctions, using the most efficient restructuring focal adhesion complex components to regulate junction restructuring to facilitate germ cell movement during spermatogenesis (for recent reviews, see Refs. 9 and 42). Needless to say, the precise mechanism(s) and interactions by which proteases and protease inhibitors regulate the epithelial cycle remain to be investigated, yet these findings have opened an unprecedented opportunity to study BTB dynamics. Moreover, proteases that are activated during the $CdCl_2$- or 1-(2,4-dichlorobenzyl)-indazole-carbohydrazide-induced damage to the seminiferous epithelium may in turn activate other cellular events besides breaking down cell junctions. For instance, it has been shown that the cleavage products of collagens by MMPs can function as biologically active peptides to regulate integrin signaling function (for a review, see Ref. 9). Such a possibility must be vigorously investigated in future studies.

BTB dynamics are regulated by multiple signaling pathways that determine the levels of different proteins and their homeostasis in the seminiferous epithelium

The results presented herein, together with earlier reports, have demonstrated that BTB dynamics in the testis are regulated by multiple pathways, which include at least two MAPK pathways, namely JNK and p38 MAPK (6, 16). It was reported that activation of the p38 MAPK pathway during $CdCl_2$-induced BTB disruption is being used to regulate the levels of occludin and ZO-1 at the BTB site (16). Subsequent studies have shown that this pathway also regulated the levels of protease cathepsin L and other AJ proteins, such as N-cadherin, β-catenin, nectin ,and afadin, at the ES and BTB sites (6). In the present study, the JNK signaling pathway was shown to be involved in junction dynamics by regulating the production of α_2-MG in a way that counteracts the disruptive effects of the p38 MAPK pathway, defending the seminiferous epithelium from the $CdCl_2$-induced disruption. The fact that p38 MAPK and JNK are having a yin-yang relationship in regulating junction dynamics in the testis is not entirely surprising because these two signal transducers are known to have differential and even opposing effects on physiological responses in other systems. For instance, they were activated differentially in the mouse brain during viral infec-

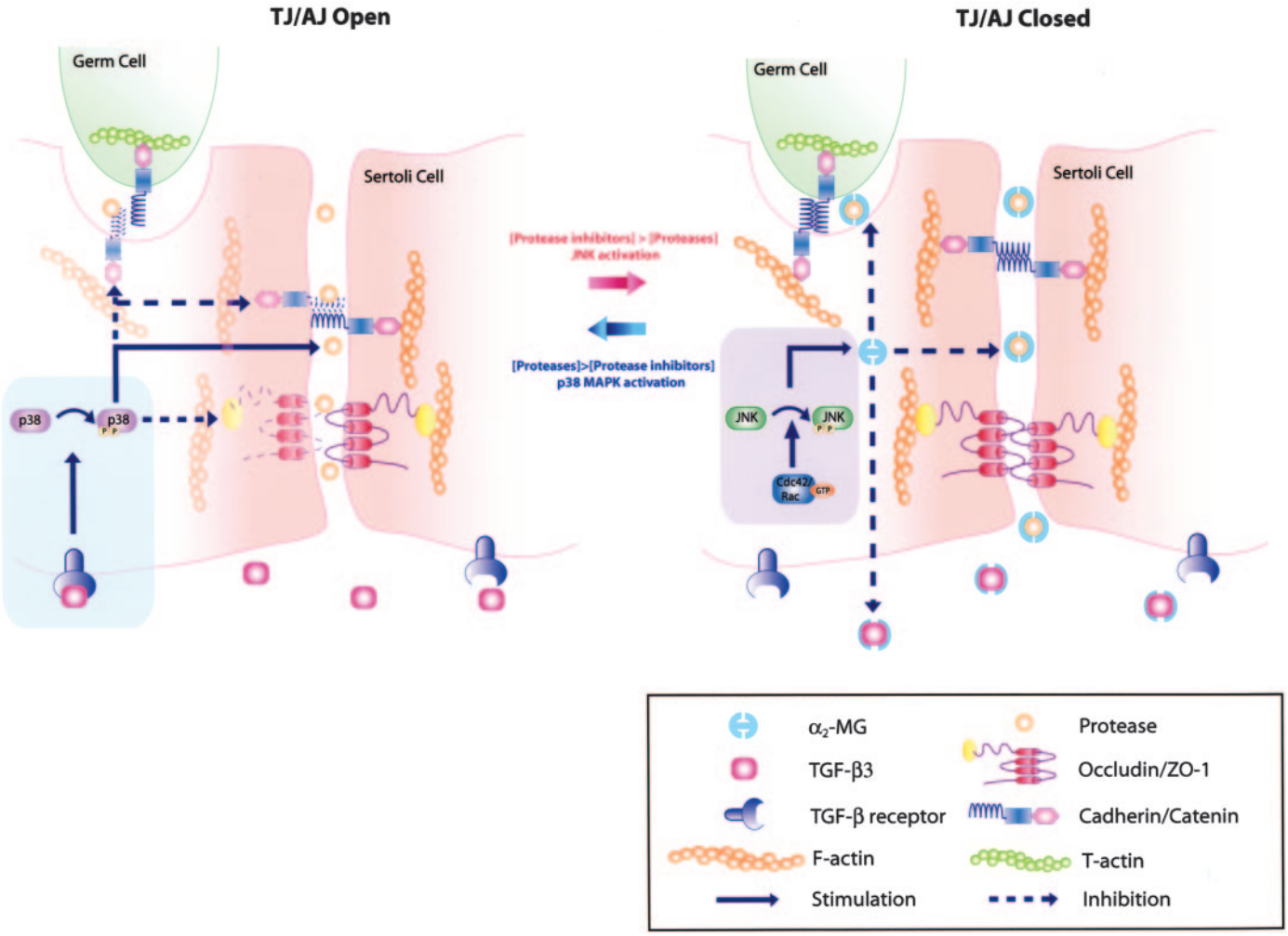

FIG. 10. A schematic drawing that illustrates the possible mechanism that regulates α_2-MG and its role in BTB restructuring in the rat testis. This schematic drawing illustrates the opening and closing of TJs and AJs (*e.g.* basal ES) in the seminiferous epithelium, which are regulated by different MAPK pathways and the steady-state α_2-MG level. Previous studies illustrated the role of TGFβ3/p38 MAPK in BTB disassembly in the testis (6, 16). When TGFβ3 binds to its receptor, the p38 MAPK pathway is activated to reduce the levels of TJ and AJ constituent proteins while promoting protease production in the seminiferous epithelium, leading to junction disassembly, opening the BTB to permit the migration of preleptotene and leptotene spermatocytes. To limit the extent of junction disruption, α_2-MG, the production of which is positively induced by JNK, binds excessive cytokines, rendering them inactive. α_2-MG also inhibits unwanted proteolysis to prevent unwanted proteolysis of TJ and AJ proteins at the cell-cell interface. This in turn favors the reassembly of the junctions, tightening the BTB.

tion by influenza A virus, playing distinctive roles during the course of this viral infection (49). Moreover, the activation of p38 MAPK in rat neonatal ventricular myocytes stimulates the production of atrial natriuretic factor, a cardiac hypertrophy marker, whereas JNK inhibits its expression in the same system (50). Thus, these two MAPKs possibly counterbalance each other to maintain a homeostasis of proteins important to junction dynamic regulation in the testis. We propose that p38 MAPK is being used to facilitate TJ-AJ disassembly, whereas JNK facilitates junction reassembly (Fig. 10). This latter mechanism likely involves α_2-MG, which inhibits unwanted proteolysis in the epithelium and binds excessive cytokines to protect Sertoli-Sertoli and Sertoli-germ cell junctions from unnecessary damages (Fig. 10).

In summary, we report herein the importance of α_2-MG in junction dynamics during spermatogenesis *in vivo* using cadmium-induced BTB damage as a model. We have also illustrated the novelty of JNK activation in maintaining TJ and AJ integrity via its effects on the homeostasis of proteases and protease inhibitors (*e.g.* α_2-MG). These findings will have significant ramification in male contraceptive development. For instance, a compromise of the homeostasis between proteases and protease inhibitors in the seminiferous epithelium will likely disrupt the migration of preleptotene and leptotene spermatocyte across the BTB. This in turn leads to male infertility.

Acknowledgments

The authors thank Ms. Eleana Sphicas (Bio-Imaging Resource Center, Rockefeller University, New York, NY) for her excellent assistance in studies using electron microscopy.

Received November 10, 2004. Accepted December 13, 2004.

Address all correspondence and requests for reprints to: C. Yan Cheng, Ph.D., Population Council, 1230 York Avenue, New York, New York 10021. E-mail: y-cheng@popcbr.rockefeller.edu.

This work was supported in part by grants from the National Institutes of Health (National Institute of Child Health and Human Development,

U01 HD045908, to C.Y.C., U54 HD029990, Project 3, to C.Y.C.) and the CONRAD Program (CICCR, CIG 01-72, to C.Y.C.; CIG 01-74, to D.D.M.).

References

1. **Johnsen M, Lund LR, Romer J, Almholt K, Dano K** 1998 Cancer invasion and tissue remodeling: common themes in proteolytic matrix degradation. Curr Opin Cell Biol 10:667–671
2. **Murphy G, Gavrilovic J** 1999 Proteolysis and cell migration: creating a path? Curr Opin Cell Biol 11:614–621
3. **Hermant B, Bibert S, Concord E, Dublet B, Weidenhaupt M, Vernet T, Gulino-Debrac D** 2003 Identification of proteases involved in the proteolysis of vascular endothelium cadherin during neurophil transmigration. J Biol Chem 278:14002–14012
4. **Mruk DD, Siu MKY, Conway AM, Lee NPY, Lau ASN, Cheng CY** 2003 Role of tissue inhibitor of metalloproteases-1 in junction dynamics in the testis. J Androl 24:510–523
5. **Wong CCS, Chung SSW, Grima J, Zhu LJ, Mruk D, Lee WM, Cheng CY** 2000 Changes in the expression of junctional and nonjunctional complex component genes when inter-Sertoli tight junctions are formed *in vitro*. J Androl 21:227–237
6. **Wong CH, Mruk DD, Lui WY, Cheng CY** 2004 Regulation of the blood-testis barrier dynamics in the testis: an *in vivo* study. J Cell Sci 117:783–798
7. **Zhu LJ, Cheng CY, Phillips DM, Bardin CW** 1994 The immunohistochemical localization of α_2-macroglobulin in rat testes is consistent with its role in germ cell movement and spermiation. J Androl 15:575–582
8. **Fritz IB, Tung PS, Ailenberg M** 1993 Proteases and antiproteases in the seminiferous tubule. In: Russell LD, Griswold MD, eds. The Sertoli cell. Clearwater, FL: Cache River; 217–235
9. **Siu MKY, Cheng CY** 2004 Dynamic cross-talk between cells and the extracellular matrix in the testis. Bioessays 26:978–992
10. **Mruk D, Zhu LJ, Silvestrini B, Lee WM, Cheng CY** 1997 Interactions of proteases and protease inhibitors in Sertoli-germ cell cocultures preceding the formation of specialized Sertoli-germ cell junctions *in vitro*. J Androl 18:612–622
11. **Sottrup-Jensen L** 1989 α-Macroglobulins: structure, shape, and mechanism of proteinase complex formation. J Biol Chem 264:11539–11542
12. **O'Connor-McCourt M, Wakefield LM** 1987 Latent transforming growth factor-β in serum. A specific complex with α_2-macroglobulin. J Biol Chem 262:14090–14099
13. **Feige JJ, Negoescu A, Keramidas M, Souchelnitskiy S, Chambaz EM** 1996 α_2-Macroglobulin: a binding protein for transforming growth factor-β and various cytokines. Horm Res 45:227–232
14. **James K** 1990 Interactions between cytokines and α_2-macroglobulin. Immunol Today 11:163–166
15. **Cheng CY, Grima J, Stahler MS, Guglielmotti A, Silvestrini B, Bardin CW** 1990 Sertoli cell synthesizes and secretes a protease inhibitor, α_2-macroglobulin. Biochemistry 29:1063–1068
16. **Lui WY, Wong CH, Mruk D, Cheng CY** 2003 TGF-β3 regulates the blood-testis barrier dynamics via the p38 mitogen activated protein (MAP) kinase pathway: An *in vivo* study. Endocrinology 144:1139–1142
17. **Setchell BP, Waites GMH** 1970 Changes in the permeability of the testicular capillaries and of the "blood-testis barrier" after injection of cadmium chloride in the rat. J Endocrinol 47:81–86
18. **Hew K, Heath GL, Jiwa AH, Welsh MJ** 1993 Cadmium *in vivo* causes disruption of tight junction-associated microfilaments in rat Sertoli cells. Biol Reprod 49:840–849
19. **Eng F, Wiebe JP, Alima LH** 1994 Long-term alterations in the permeability of the blood-testis barrier following a single intratesticular injection of dilute aqueous glycerol. J Androl 15:311–317
20. **Grima J, Wong CCS, Zhu LJ, Zong SD, Cheng CY** 1998 Testin secreted by Sertoli cells is associated with the cell surface, and its expression correlates with the disruption of Sertoli-germ cell junctions but not the inter-Sertoli tight junction. J Biol Chem 273:21040–21053
21. **Russell LD, Sexana NK, Weber JE** 1987 Intratesticular injection as a method to assess the potential toxicity of various agents to study mechanisms of normal spermatogenesis. Gamete Res 17:43–56
22. **Bradford MM** 1976 A rapid and sensitive method for the quantitation of microgram quantities of protein utilizing the principle of protein-dye binding. Anal Biochem 72:248–254
23. **Sato F, Matsukawa U, Matsumoto K, Nishino H, Sakai T** 1994 Apigenin induces morphological differentiation and G_2-M arrest in rat neuronal cells. Biochem Biophys Res Commun 204:578–584
24. **Ravanti L, Heino J, Lopez-Otin C, Kahari VM** 1999 Induction of collagenase-3 (MMP-13) expression in human skin fibroblasts by three dimensional collagen is mediated y p38 mitogen-activated protein kinase. J Biol Chem 274:2446–2455
25. **Favata MF, Horiuchi KY, Manos EJ, Daulerio AJ, Stradley DA, Feeser WS, Van Dyk DE, Pitts WJ, Earl RA, Hobbs F, Copeland RA, Magolda RL, Scherle PA, Trzaskos JM** 1998 Identification of a novel inhibitor of mitogen-activated protein kinase. J Biol Chem 273:18623–18632
26. **De Cesaris P, Starace D, Starace G, Filippini A, Stefanini M, Ziparo E** 1999 Activation of Jun N-terminal kinase/stress-activated protein kinase pathway by tumor necrosis factor α leads to intercellular adhesion molecule-1 expression. J Biol Chem 274:28978–28982
27. **Northemann W, Heisig M, Kunz D, Heinrich PC** 1985 Molecular cloning of cDNA sequences for rat α_2-macroglobulin and measurement of its transcription during experimental inflammation. J Biol Chem 260:6200–6205
28. **Northemann W, Andus T, Gross V, Heinrich PC** 1983 Cell-free synthesis of rat α_2-macroglobulin and induction of its mRNA during experimental inflammation. Eur J Biochem 137:257–262
29. **Andus T, Geiger T, Hirano T, Kishimoto T, Tran-Thi TA, Decker K, Heinrich PC** 1988 Regulation of synthesis and secretion of major rat acute-phase proteins by recombinant human interleukin-6 (BSF-2/IL-6) in hepatocyte primary cultures. Eur J Biochem 173:287–293
30. **Ganter U, Strauss S, Jonas U, Weidemann A, Beyreuther K, Volk B, Berger M, Bauer J** 1991 α2-Macroglobulin synthesis in interleukin-6-stimulated human neuronal (SH-SY5Y neuroblastoma) cells. Potential significance for the processing of Alzheimer β-amyloid precursor protein. FEBS Lett 282:127–131
31. **Shi DL, Savona C, Gagnon J, Cochet C, Chambaz EM, Feige JJ** 1990 Transforming growth factor-β stimulates the expression of α_2-macroglobulin by cultured bovine adrenocortical cells. J Biol Chem 265:2881–2887
32. **Fabrizi C, Colasanti M, Persichini T, Businaro R, Starace G, Lauro GM** 1994 Interferon γ up-regulates α_2-macroglobulin expression in human astrocytoma cells. J Neuroimmunol 53:31–37
33. **Zwain IH, Grima J, Stahler MS, Saso L, Cailleau J, Verhoeven G, Bardin CW, Cheng CY** 1993 Regulation of Sertoli cell α_2-macroglobulin and clusterin (SGP-2) secretion by peritubular myoid cells. Biol Reprod 48:180–187
34. **Stahler MS, Schlegel P, Bardin CW, Silvestrini B, Cheng CY** 1991 α_2-Macroglobulin is not an acute-phase protein in the rat testis. Endocrinology 128:2805–2814
35. **Braghiroli L, Silvestrini B, Sorretino C, Grima J, Mruk D, Cheng CY** 1998 Regulation of α_2-macroglobulin expression in rat Sertoli cells and hepatocytes by germ cells *in vitro*. Biol Reprod 59:111–123
36. **Li AHY, Zwain IH, Pineau C, Cazzolla N, Saso L, Silvestrini B, Bardin CW, Cheng CY** 1994 Response of α_2-macroglobulin messenger ribonucleic acid expression to acute inflammation in the testis is different from the response in the liver and brain. Biol Reprod 50:1287–1296
37. **Siu MKY, Cheng CY** 2004 Extracellular matrix: recent advances on its role in junction dynamics in the seminiferous epithelium during spermatogenesis. Biol Reprod 71:375–391
38. **Lui WY, Mruk D, Lee WM, Cheng CY** 2003 Sertoli cell tight junction dynamics: their regulation during spermatogenesis. Biol Reprod 68:1087–1097
39. **Marino MW, Dunbar JD, Wu LW, Ngaiza JR, Ham HM, Guo D, Matsushita M, Narin AC, Zhang Y, Kolesnick R, Jaffe EA, Donner DB** 1996 Inhibition of tumor necrosis factor signal transduction in endothelial cells by dimethylaminopurine. J Biol Chem 271:28624–28629
40. **Ryden M, Dicker A, van Harmelen V, Hauner H, Brunnberg M, Perbeck L, Lonnqvist F, Arner P** 2002 Mapping of early signaling events in tumor necrosis factor-α-mediated lipolysis in human fat cells. J Biol Chem 277:1085–1091
41. **Skinner MK** 1993 Secretion of growth factors and other regulatory factors. In: Russell LD, Griswold MD, eds. The Sertoli cell. Clearwater, FL: Cache River; 478–483
42. **Mruk DD, Cheng CY** 2004 Sertoli-Sertoli and Sertoli-germ cell interactions and their significance in germ cell movement in the seminiferous epithelium during spermatogenesis. Endocr Rev 25:747–806
43. **Lui WY, Lee WM, Cheng CY** 2003 TGF-βs: their role in testicular function and Sertoli cell tight junction dynamics. Int J Androl 26:147–160
44. **Umans L, Serneels L, Overbergh L, Lorent K, Van Lauven F, Van de Berghe H** 1995 Targeted inactivation of the mouse α_2-macroglobulin gene. J Biol Chem 270:19778–19785
45. **Umans L, Serneels L, Overbergh L, Stas L, Van Lauven F** 1999 α_2-Macroglobulin- and murinoglobulin-1-deficient mice. A mouse model for acute pancreatitis. Am J Pathol 155:983–993
46. **Streuli C** 1999 Extracellular matrix remodellng and cellular differentiation. Curr Opin Cell Biol 11:634–640
47. **Tryggvason K, Hoyhtya M, Salo T** 1987 Proteolytic degradation of extracellular matrix in tumor invasion. Biochim Biophys Acta 907:191–217
48. **Siu MKY, Cheng CY** 2004 Interactions of proteases, protease inhibitors, and the β1 integrin/laminin γ3 protein complex in the regulation of ectoplasmic specialization dynamics in the rat testis. Biol Reprod 70:945–964
49. **Mori I, Goshima F, Koshizuka T, Koide N, Sugiyama T, Yoshida T, Yokochi T, Nishiyama Y, Kimura Y** 2003 Differential activation of c-Jun N-terminal kinase/stress activated protein kinase and p38 mitogen-activated protein kinase signal transduction pathways in the mouse brain upon infection with neurovirulent influenza A virus. J Gen Virol 84:2401–2408
50. **Nemoto S, Sheng Z, Lin A** 1998 Opposing effects of Jun kinase and p38 mitogen-activated protein kinases on cardiomyocyte hypertrophy. Mol Cell Biol 18:3518–3526